Thermochimica Acta 483 (2009) 29–35

Contents lists available at ScienceDirect

Thermochimica Acta

journal homepage: www.elsevier.com/locate/tca

Synthesis and characterization of chromium doped boehmite nanofibres

Jing (Jeanne) Yang[a], Ray L. Frost[a,*], Yong Yuan[a,b]

[a] Inorganic Materials Research Program, School of Physical and Chemical Sciences, Queensland University of Technology, GPO Box 2434, Brisbane Queensland 4001, Australia
[b] Institute of Solid State Physics, Chinese Academy of Sciences, Hefei 230031, China

ARTICLE INFO

Article history:
Received 8 September 2008
Received in revised form 27 October 2008
Accepted 28 October 2008
Available online 6 November 2008

Keywords:
Boehmite
Chromium doping
Nanofibres
Nanomaterial
Transmission electron microscopy
Thermal analysis
Thermogravimetry

ABSTRACT

Thermogravimetric and differential thermogravimetric analysis has been used to study synthesised chromium doped boehmite. The dehydroxylation temperature increases significantly from 0 to 5% doping, after which the dehydroxylation temperature shows a small steady increase up to the 20% doping level. The temperature of dehydroxylation increases with time of hydrothermal treatment. Chromium doped boehmite nanofibres were also characterised by X-ray diffraction and transmission electron microscopy. Hydrothermal treatment of doped boehmite with chromium resulted in the formation of nanofibres over a wide dopant range. Nanofibres up to 500 nm in length and between 4 and 6 nm in width were produced.

1. Introduction

Compared to their micro and macro counterparts, nanosized materials have received wider attention because of their intrinsic properties, which are determined by their composition, size, shape, and structure [1]. Nanosized materials such as nanofibers, nanotubes, nanoribbons and nanorods, one dimensional (1D) nanoscale inorganic materials have attracted intensive interest due to their distinctive geometries, novel physical and chemical properties, and the potential applications in many fields. [2] Boehmite (γ -AlOOH) and its oxide derivatives such as α-Al_2O_3 and γ -Al_2O_3 have been studied extensively because they can be used as catalysts, adsorbents, flame retardants and optical materials [3–6].

Synthesis forms an essential component of nanoscience and nanotechnology. While nanomaterials have been generated by physical methods such as laser ablation, arc-discharge and evaporation, chemical methods have proved to be more effective, as they provide better control as well as enable different sizes, shapes and functionalization. Among these methods, hydrolysis and precipitation are the most common. John Bugosh first synthesised the boehmite nanofibers by a hydrothermal method in 1961 [7]. Since then, numerous studies on boehmite nanofibers have been undertaken, for example, boehmite (AlOOH) nanofibers were reported to be assembled with the assistance of poly(ethylene oxide) (PEO) surfactant [8] and tubular γ -Al_2O_3 was fabricated via soft solution route using *N*-cetyl-*N*,*N*,*N*-trimethylammonium bromide (CTAB) surfactant [9]. Shen et al. published a report showing a steam-assisted solid-phase conversion of amorphous aluminium hydroxides wet gel to well crystallised 1D nanostructure of boehmite AlOOH nanorods without using surfactants and solvents [10]. The process is unique in the simplicity of preparation and the high efficiency of crystal growth, which can be operated at a large scale.

As for doping clays, the addition of other metal ions into boehmite, especially into nanostructured boehmite would have great potential to contribute the further application of these inorganic nanomaterials due to the enhancement of its properties, and there have been reports on boehmite doped by Fe, Ga and Eu [11–13]. It is also reported that materials doped with chromium could obtain special electric, magnetic or optical properties and gain more application [14–17]. This paper reports our research on Cr-doped boehmite. Such concepts have not been previously reported.

Thermal analysis has been proved as the most useful method for the analysis of minerals and related materials. In this work, boehmite nanofibers based on Shen's methodology [10] were synthesised by introducing chromium as dopant and a series of chromium doped boehmite nanofibers with different chromium

* Corresponding author. Tel.: +61 7 3138 2407; +61 7 3138 1804.
E-mail address: r.frost@qut.edu.au (R.L. Frost).

0040-6031/$ – see front matter © 2008 Elsevier B.V. All rights reserved.
doi:10.1016/j.tca.2008.10.024

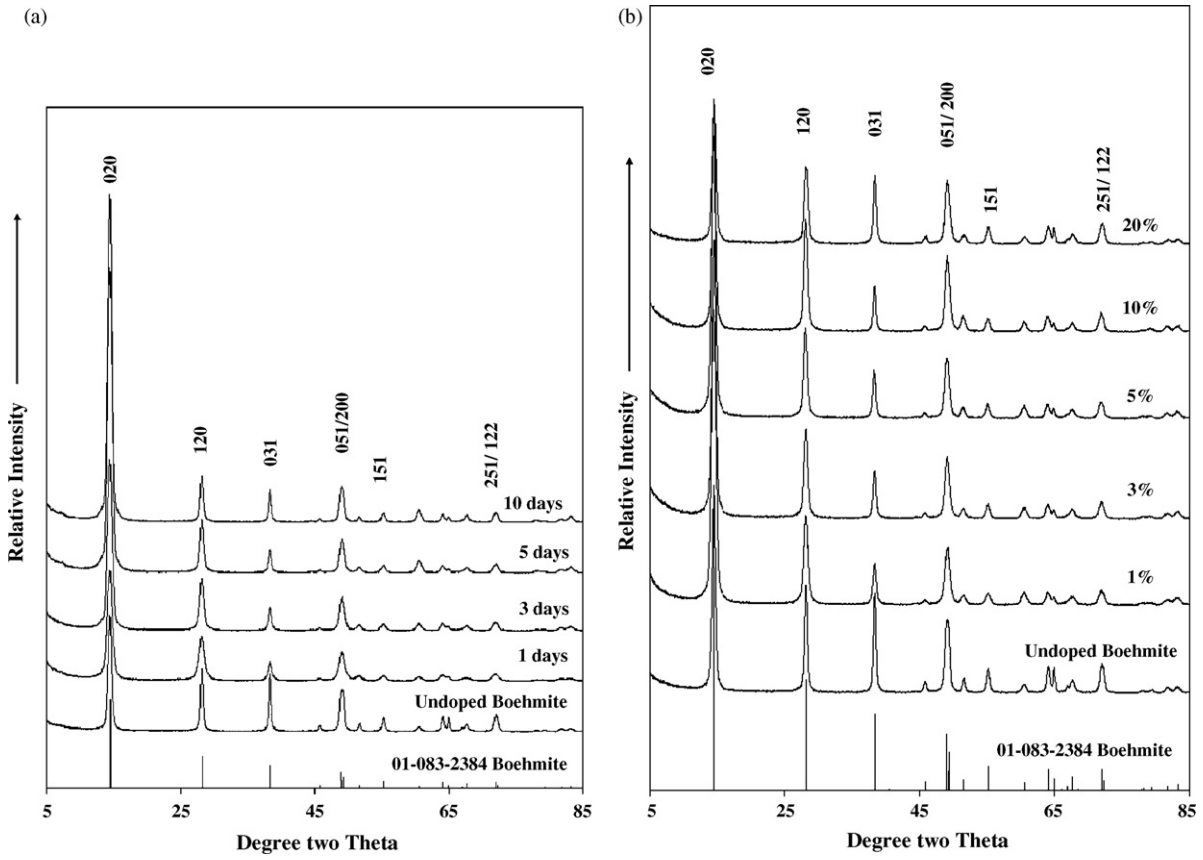

Fig. 1. (a) XRD patterns of undoped boehmite and 1% Cr-doped boehmite nanofibers with different hydrothermal treatment time at 170 °C. (b) XRD patterns of undoped boehmite and various Cr % doped boehmite nanofibers, after hydrothermal treatment at 170 °C for 3 days.

content percentage and varying hydrothermal treatment time have been systematically studied with the thermo gravimetric techniques.

2. Experimental

2.1. Synthesis of chromium doped boehmite nanofibers

A total amount of 0.02 moles of aluminium nitrate and chromium nitrate was mixed before being dissolved in ultra-pure water. To make a comparison, mixtures with chromium molar percentage of 0, 1, 3, 5, 10 and 20% were prepared separately and then dissolved in ultra-pure water to form solutions with a metal ion to H_2O molar ratio of 1:35. At room temperature, 10% by weight ammonia solution was added dropwise into the metal ions solution while stirring vigorously. The addition of the ammonia solution was ceased when the pH value of the reaction mixture reached 5. The mixture was then stirred at room temperature for 1 h. The obtained gel was filtrated to obtain the wet gel-cake, which was then transferred into a 25 mL glass beaker. Before putting the beaker with gel-cake into a Teflon vessel (125 mL), 2 ml ultrapure water was poured to the bottom of each vessel separately. The Teflon vessels were sealed and heated at 170 °C for 1, 3, 5 and 10 days. The resulting materials were washed several times with ultrapure water, centrifuged, and dried in air at 35 °C for 2 days.

2.2. X-ray diffraction

XRD analyses were performed on a PANalytical X'Pert PRO X-ray diffractometer (radius: 240.0 mm). Incident X-ray radiation was produced from a line focused PW3373/10 Cu X-ray tube, operating at 40 kV and 40 mA, wavelength of 1.54 Å.

2.3. TEM analysis

A Philips CM 200 transmission electron microscopy (TEM) at 200 kV was used to investigate the morphology of the boehmite nanofibers. All samples were dispersed in absolute ethanol solution and then dropped on copper grids.

2.4. Thermal analysis

Thermal decomposition of the Cr-doped boehmite was carried out in a TA® Instrument incorporating a high-resolution thermo gravimetric analyser (series Q500) in a flowing nitrogen atmosphere (60 cm^3 min^{-1}). Approximately 20 mg of each sample underwent thermal analysis, with a heating rate of 5 °C/min, with resolution of 6 from 25 to 1000 °C. With the isothermal, isobaric heating program of the instrument, the furnace temperature was regulated precisely to provide a uniform rate of decomposition in the main decomposition stage.

3. Results and discussion

3.1. X-ray diffraction

X-ray diffraction was normally used to determine the phase and purity of the synthesised materials. Fig. 1a and b displays well-defined XRD patterns observed and all diffraction peaks were perfectly indexed to the XRD pattern of undoped boehmite

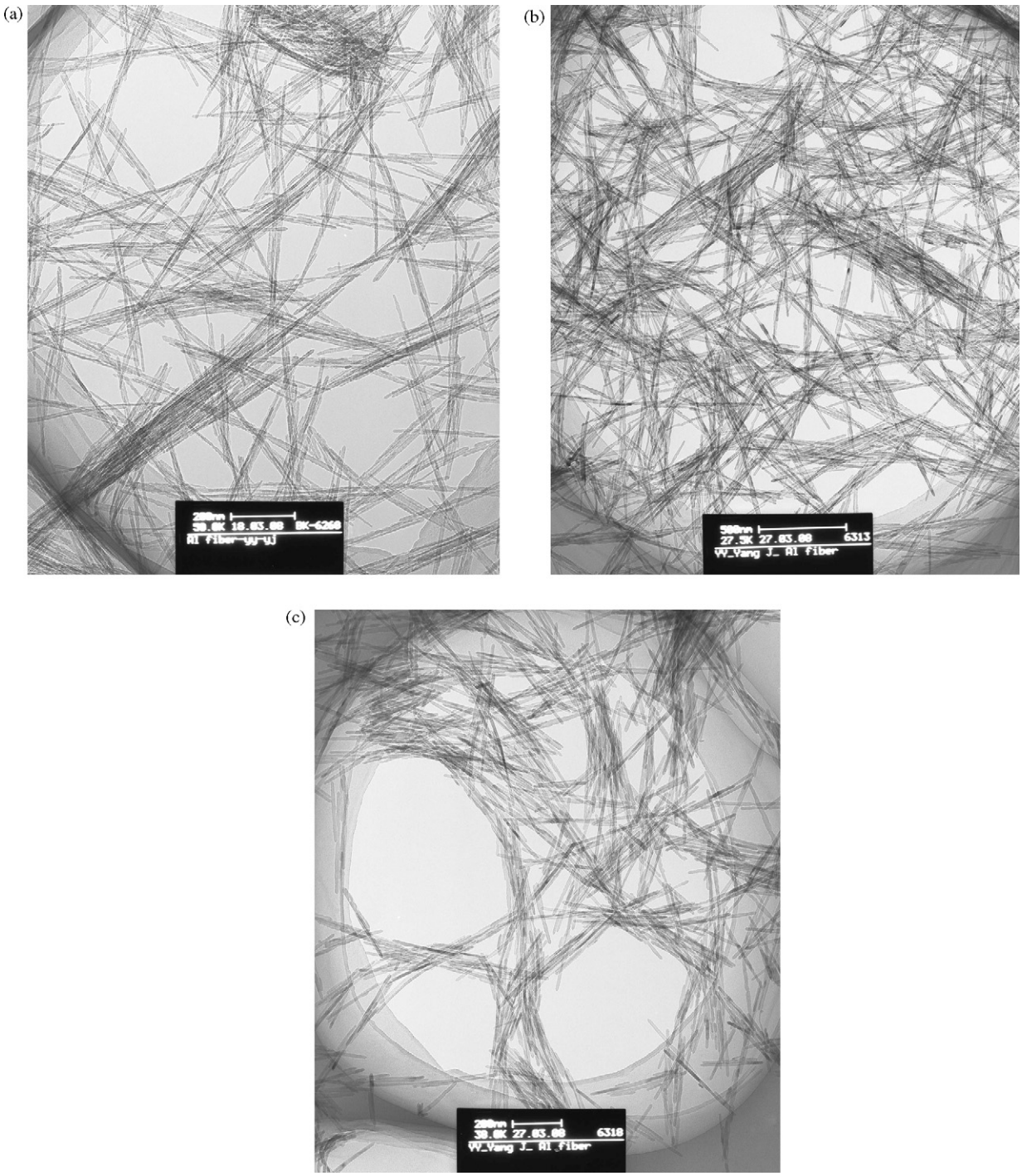

Fig. 2. TEM images of the synthetic nanofibers with 3-day hydrothermal treatment: (a) undoped boehmite, (b) 3% Cr-doped and (c) 5% Cr-doped.

(JCPDS card 01-083-2384). No XRD peaks representing other crystalline phases were detected, indicating that the chromium doped nanofibers of the synthetic boehmite exhibited excellent crystallinity and a high purity. Fig. 1a shows that the peaks are higher and narrower with the increase of the hydrothermal treatment time to 10 days, which means the crystals grew better as synthesis time getting longer.

3.2. Transmission electron microscopy

The transmission electron microscopy images of the synthesised undoped and Cr-doped boehmite are shown in Fig. 2. The figure shows the TEM images of (a) undoped boehmite, (b) 3% Cr-doped and (c) 5% Cr-doped. The figure clearly shows that the boehmite is fibrous with very long narrow fibres often exceeding 500 nm in length and with width of between 2 and 6 nm. Many of the fibres are curved or bent as may be observed in Fig. 2c for the 5% Cr-doped boehmite.

3.3. Thermogravimetric analysis

The thermogravimetric analysis and the differential thermal analysis of nanostructured undoped boehmite and doped boehmite with varying amounts of chromium dopant from 0 to 20% are

shown. The thermal analysis pattern of undoped boehmite is displayed in Fig. 3a. Fig. 3b reports the effect of hydrothermal treatment time on the formation of boehmite nanofibres. Fig. 4 shows the effect of the % of doping on the thermal analysis of Cr doped boehmite. The results of the thermal analyses are summarised in Table 1.

The TG of the undoped boehmite shows a strongly asymmetric curve with a peak temperature of 406.5 °C and a mass loss of 15.8%. The thermal decomposition occurs as follows: $2AlO(OH) \rightarrow Al_2O_3 + H_2O$. This major decomposition step is attributed to the dehydroxylation of the boehmite**.** Two low mass loss steps at 45 and 260 °C with mass losses of 1.5 and 1.7% are also observed. The first mass loss step is assigned to the dehydration of boehmite (Column 1 in Table 1)

The thermal decomposition of 1% doped boehmite with 1 day hydrothermal treatment shows three mass loss steps at 46, 311

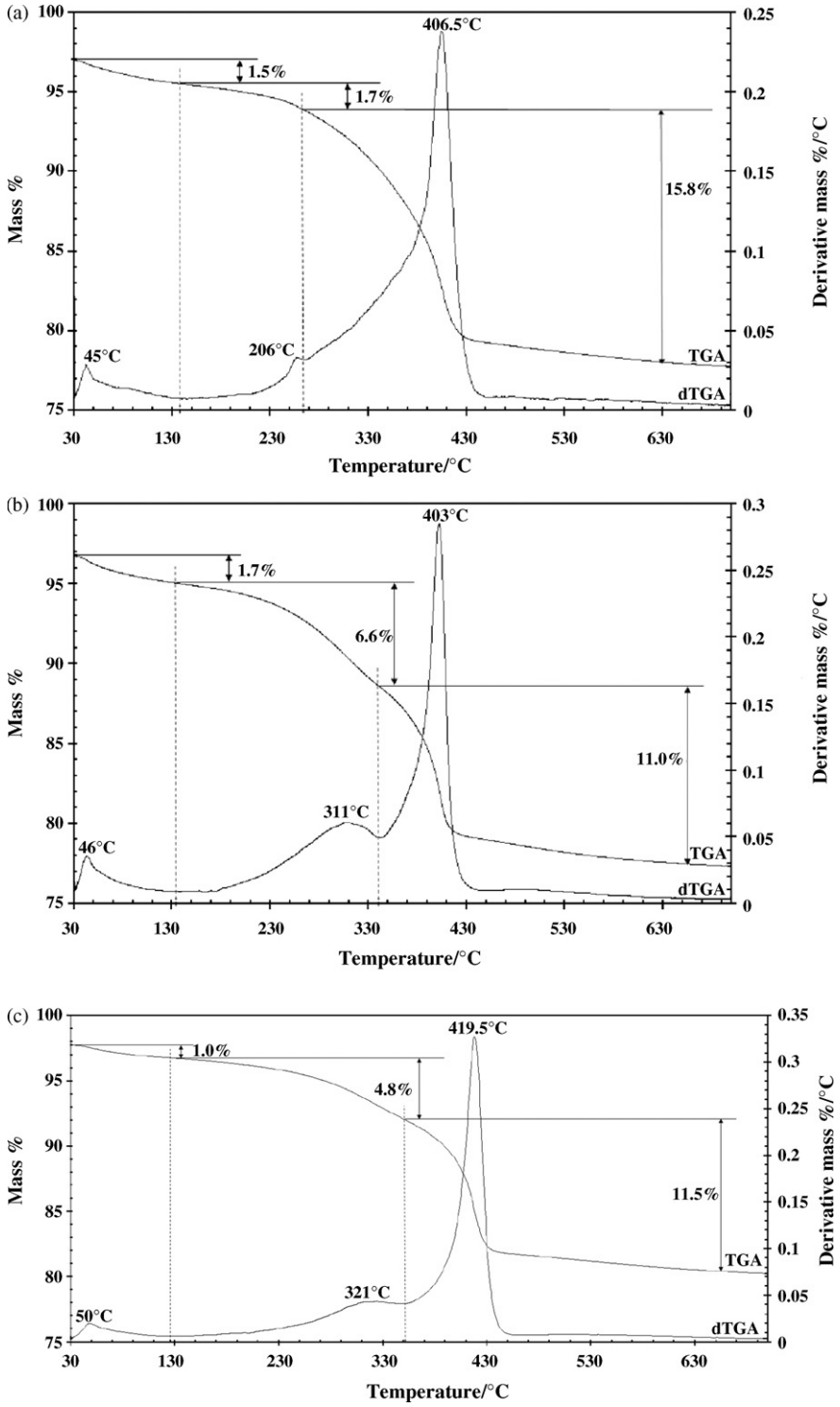

Fig. 3. Thermal analysis patterns of (a) undoped boehmite nanofibres and 1% Cr doped boehmite nanofibers with different hydrothermal treatment time: (b) 1 day, (c) 3 days, (d) 5 days, and (e) 10 days.

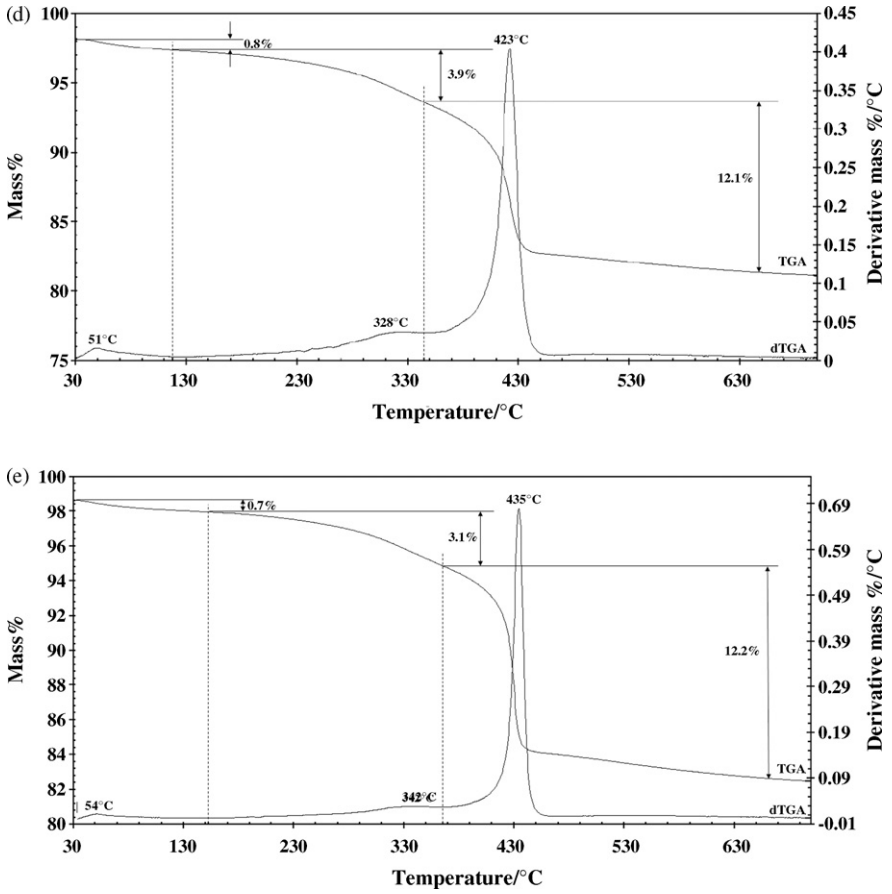

Fig. 3. (*Continued*).

and 403 °C with mass losses of 1.7, 6.6 and 11.0% (Fig. 3b). The asymmetry observed in Fig. 3a is no longer observed but a second peak at 311 °C is found. The thermal decomposition of 1% doped boehmite with 3 day hydrothermal treatment shows three mass loss steps at 50, 321 and 419.5 °C with mass losses of 1.0, 4.8 and 11.5% (Fig. 3c). The thermal decomposition of 1% doped boehmite with 5 day hydrothermal treatment shows three mass loss steps at 51, 328 and 423 °C with mass losses of 0.8, 3.9 and 12.1% (Fig. 3d). The results of the 1% Cr doped boehmite hydrothermally treated for 10 days (Fig. 3e) shows a large mass loss step at 435 °C with a mass loss of 12.2%. In addition two smaller mass loss steps at 54 and 342 °C with mass losses of 0.7 and 3.1% are observed. It is apparent that thermal decomposition temperature of the Cr doped boehmite varies with the hydrothermal treatment time. This variation is reported in Fig. 5.

The variation in the % chromium doping on the thermal analysis patterns and decomposition of boehmite is explored in Fig. 4a–d. The thermal analysis patterns of 3% Cr doped boehmite hydrothermally treatment for 3 days shows three mass loss steps at 46, 315 and 427 °C with mass losses of 1.1, 2.9, and 12.4%. The dehydroxylation peak at 427 °C is sharp indicating that the dehydroxylation occurs over a very narrow temperature range. For the 5% Cr doped boehmite the dehydroxylation step is observed at 430.5 °C with a mass loss of 13.1%. For the 10% Cr doped boehmite hydrothermally treated for 3 days results in a sharp mass loss peak at 433 °C with minor mass loss steps at 50 and 380 °C. The temperature for the Cr 20% doped boehmite is 436.5 °C. The variation in the temperature of the decomposition of boehmite as a function of % doping is reported in Fig. 6. It is apparent that as the % of Cr is increased in the boehmite the dehy-

Table 1
Results of the thermal analysis of the undoped and various % Cr doped boehmite nanofibers.

Sample	Decomposition steps			Peaks			Total mass loss
	Step 1	Step 2	Step 3	Peak 1	Peak 2	Peak 3	
Boehmite	1.5%	1.7%	15.8%	45 °C	260 °C	406.5 °C	19.0%
1% – 1 d	1.7%	6.6%	11.0%	46 °C	311 °C	403 °C	19.3%
1% – 3 d	1.0%	4.8%	11.5%	50 °C	321 °C	419.5 °C	17.3%
1% – 5 d	0.8%	3.9%	12.1%	51 °C	328 °C	423 °C	16.8%
1% – 10 d	0.7%	3.1%	12.2%	54 °C	342 °C	435 °C	16.0%
3% – 3 d	1.1%	2.9%	12.4%	46 °C	315 °C	427 °C	16.4%
5% – 3 d	0.8%	2.1%	13.1%	48 °C	325 °C	430.5 °C	16.0%
10% – 3 d	0.8%	–	15.1%	50 °C	380 °C	433 °C	15.9%
20% – 3 d	1.0%	–	15.0%	50 °C	330 °C	436.5 °C	16.0%

*"d" means "days of hydrothermal treatment".

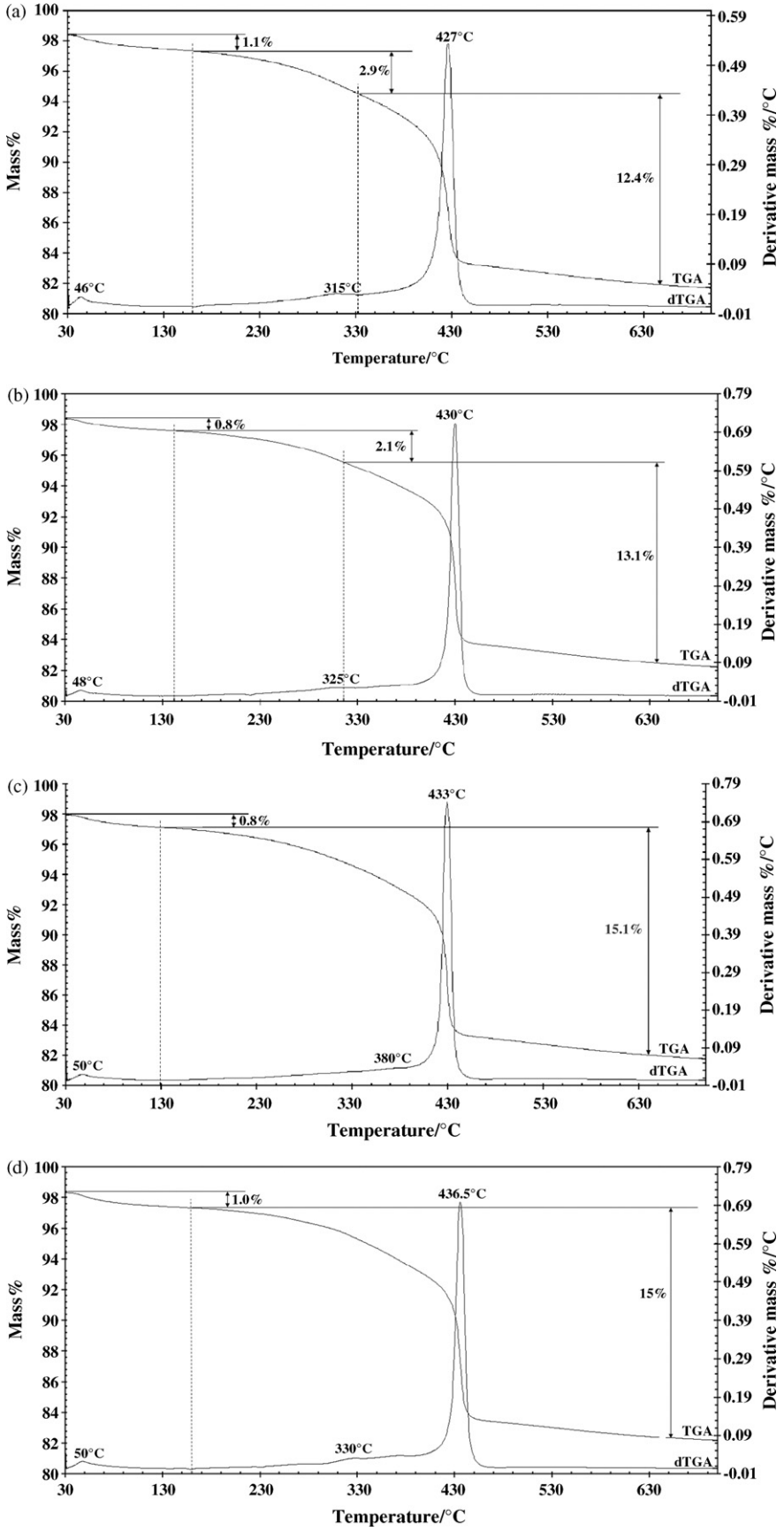

Fig. 4. Thermal analysis patterns of various % Cr-doped boehmite nanofibers with 3-day hydrothermal treatment: (a) 3%, (b) 5%, (c) 10%, and (d) 20%.

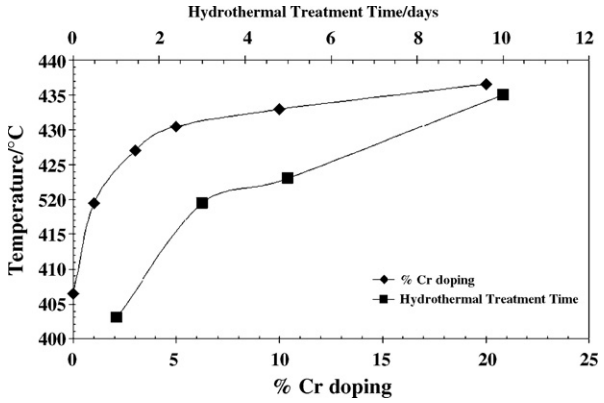

Fig. 5. Dehydroxylation temperature of the DTG peak as a function of added Cr content and with the hydrothermal treatment time.

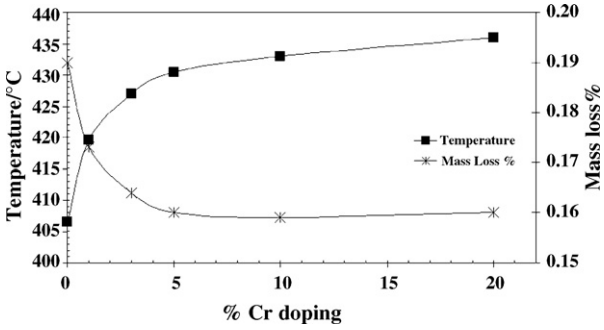

Fig. 6. Temperature of the main dTGA peak and the total mass loss percentage as a function of added Cr content.

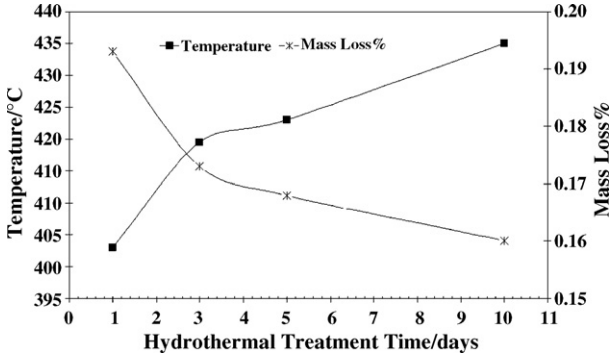

Fig. 7. Temperature of the main dTGA peak and the total mass loss percentage as a function of the hydrothermal treatment time.

droxylation temperature is increased and shifts from 406.5 to 436.5 °C.

The variation of the dehydroxylation temperature and associated mass loss with the % of Cr doping is shown in Fig. 6. As the dehydroxylation temperature increases the mass loss from the dehydroxylation step decreases. The dehydroxylation temperature increases significantly from 0 to 5% doping, after which the dehydroxylation temperature shows a small steady increase up to the 20% doping level. The associated mass loss decreases and then shows a constant mass loss. The variation of mass loss and dehydroxylation temperature with hydrothermal treatment time is illustrated in Fig. 7. The temperature of dehydroxylation increases with time of hydrothermal treatment.

4. Conclusions

Boehmite and chromium doped boehmite were synthesised by low temperature precipitation from aqueous solution and hydrothermally treated for differing time intervals. Very long nanofibres were produced often exceeding 500 nm in length. Normally at above the 5% doping level a mixture of nanofibres are produced.

Doping with chromium resulted in an increase in the dehydroxylation temperature of boehmite from ~406.5 to 436.5 °C. The temperature of dehydroxylation increases with time of hydrothermal treatment. The dehydroxylation temperature increases significantly from 0 to 5% doping, after which the dehydroxylation temperature shows a small steady increase up to the 20% doping level.

Acknowledgements

The financial and infra-structure support of the Queensland University of Technology Inorganic Materials Research Program of the School of Physical and Chemical Sciences is gratefully acknowledged. The Australian Research Council (ARC) is thanked for funding the instrumentation.

References

[1] Y.G. Sun, Y.N. Xia, Science 298 (2002) 2176–2179.
[2] M.S. Gudiksen, L.J. Lauhon, J. Wang, D.C. Smith, C.M. Lieber, Nature 415 (2002) 617–620.
[3] D. Mishra, S. Anand, R.K. Panda, R.P. Das, Materials Letters 42 (2000) 38–45.
[4] V.S. Burkat, V.S. Dudorova, V.S. Smola, T.S. Chagina, Light Metals, Warrendale, PA, United States, 1985, pp. 1443–1448.
[5] J.-L. Le Loarer, H. Nussbaum, D. Bortzmeyer, Alumina extrudates, methods for preparing and use as catalysts or catalyst supports. (Rhodia Chimie, Fr.). Application: WO, 1998, p. 44.
[6] C. Nedez, J.-P. Boitiaux, C.J. Cameron, B. Didillon, Langmuir 12 (1996) 3927–3931.
[7] J. Bugosh, Journal of Physical Chemistry 65 (1961) 1789–1792.
[8] H.Y. Zhu, X.P. Gao, D.Y. Song, Y.Q. Bai, S.P. Ringer, Z. Gao, Y.X. Xi, W. Martens, J.D. Riches, R.L. Frost, Journal of Physical Chemistry B 108 (2004) 4245–4247.
[9] D. Kuang, Y. Fang, H. Liu, C. Frommen, D. Fenske, Journal of Materials Chemistry 13 (2003) 660–662.
[10] S.C. Shen, Q. Chen, P.S. Chow, G.H. Tan, X.T. Zeng, Z. Wang, R.B.H. Tan, Journal of Physical Chemistry C 111 (2007) 700–707.
[11] Y.Y. Zhao, W.N. Martens, T.E. Bostrom, H.Y. Zhu, R.L. Frost, Langmuir 23 (2007) 2110–2116.
[12] Y.Y. Zhao, R.L. Frost, W.N. Martens, Journal of Physical Chemistry C 111 (2007) 5313–5324.
[13] J.M.A. Caiut, S.J.L. Ribeiro, Y. Messaddeq, J. Dexpert-Ghys, M. Verelst, H. Dexpert, Nanotechnology 18 (2007).
[14] K. Fujita, Y. Tokudome, K. Nakanishi, K. Miura, K. Hirao, Journal of Non-Crystalline Solids 354 (2008) 659–664.
[15] Y.C. Huang, J.S. Wang, Y.K. Lu, W.K. Liu, K.Y. Huang, S.L. Huang, W.H. Cheng, Optics Express 15 (2007) 14382–14388.
[16] C.G. Jin, X.M. Wu, L.J. Zhuge, Z.D. Sha, B. Hong, Journal of Physics D-Applied Physics 41 (2008).
[17] S.M. Abo-Naf, M.S. El-Amiry, A.A. Abdel-Khalek, Optical Materials 30.